THE JOURNAL OF CHEMICAL PHYSICS 134, 194306 (2011)

The infrared spectra of BF_3^+ and BF_2OH^+ trapped in solid neon

Marilyn E. Jacox[a] and Warren E. Thompson[b]
Optical Technology Division, National Institute of Standards and Technology, Gaithersburg, Maryland 20899-8441, USA

(Received 10 March 2011; accepted 15 April 2011; published online 18 May 2011)

Observations on a Ne:BF_3 = 400:1 mixture into which a trace of normal or isotopically enriched water had been introduced, codeposited at 4.3 K with a beam of neon atoms that had been excited in a microwave discharge, demonstrate that a pair of absorptions at 1662 cm^{-1} and 1722 cm^{-1} that were previously assigned to the two boron-isotopic species of BF_3^+ should be reassigned to a BF_2 stretching fundamental of BF_2OH^+. The OH stretching fundamental of that product was identified for the first time at 3240 cm^{-1}. The degenerate BF_3 stretching fundamental of $^{11}BF_3^+$ appears at an unusually high frequency, 1790 cm^{-1}, consistent with strong *pseudo*-Jahn-Teller interaction of that ground-state fundamental with the $\tilde{B}^2E'$ electronic state, as predicted by theory. The recent availability of detailed *ab initio* and density functional calculations of the vibrational fundamentals of BF_2^- and BF_3^- facilitates assignment of the infrared absorptions of those two products. [doi:10.1063/1.3587133]

I. INTRODUCTION

Despite the fundamental importance of the properties of the molecular fragments and ions derived from BF_3 and the widespread use of discharges through BF_3 in microcircuit fabrication, little is known about the structure and spectroscopy of these species.

Some of the gaps in our knowledge of these properties were filled by an earlier study in this laboratory of the infrared spectra of the products of the codeposition of a very dilute mixture of BF_3 in neon at 4.3 K with a beam of neon atoms that had been excited in a microwave discharge.[1] Assignments were obtained for infrared absorptions of BF_3^+, BF_2, BF_2^+, and BF_3^-, each of which had a distinctive photodestruction behavior when the initial deposit was exposed to filtered radiation in the visible and near ultraviolet spectral region.

Subsequent related studies of other heavily fluorinated compounds, several of which–such as BF_3–have high first ionization energies, indicated that oxygen-containing products are commonly formed. PF_3 and PF_5 both react readily with H_2O adsorbed on the walls of the vacuum system to form PF_3O, the infrared absorptions of which were quite prominent in all of the experiments.[2] Also identified in the solid deposit were infrared absorptions of F_3PO^-, F_2PO, F_2PO^+, FPO, and, tentatively, F_2PO^-. Other experiments on dilute mixtures of SF_4 in a large excess of neon indicated that F_2SO was present in the SF_4 sample.[3] Addition of a small amount of $H_2{}^{18}O$ to the Ne:SF_4 mixture led to the appearance of absorptions of $F_2S^{18}O$ and, in the discharge sampling study, of an absorption of $F_2S^{18}O^+$.

In the early experiments on BF_3,[1] a number of prominent, unidentified absorptions were present even in a simple Ne:BF_3 deposit without the introduction of discharge-excited neon atoms. The possibility that these resulted from reaction of BF_3 with H_2O adsorbed on the walls of the vacuum system was suggested not only by the observations on Ne:PF_n and Ne:SF_n samples but also by the earlier report by Takeo and Curl,[4] who identified the microwave spectrum of BF_2OH, produced by the reaction of BF_3 with H_2O adsorbed on the walls of their vacuum system. New experiments on Ne:BF_3:H_2O samples which were not exposed to discharged neon atoms revealed that these unidentified infrared absorptions were contributed by eight of the nine ground-state vibrational fundamentals of BF_2OH.[5] Subsequent high-resolution analyses[6] of most of the vibrational fundamentals of gas-phase BF_2OH demonstrated that the largest deviation of a neon-matrix absorption maximum from the corresponding gas-phase band center amounts to only 3.3 cm^{-1}.

Several questions are posed by the results of the two earlier studies.[1,5] First, since FBO was present and BF_2OH was later found to be an important species in the Ne:BF_3 experiments and since both uncharged and ionic oxygen-containing species were later identified in studies of ions derived from other inorganic fluorides, possibly oxygen-containing ions also contributed to the spectrum of Ne:BF_3 samples codeposited with discharged neon atoms. The assignment of infrared absorptions at both 1661.6 and 1790.4 cm^{-1} to BF_3^+ also encounters some difficulty. Most 23-valence-electron XY_3 molecules have a planar, threefold symmetric (D_{3h}) structure, implying only one infrared-active BF stretching mode. This would exclude the contribution of both of these absorptions by stretching fundamentals of $^{11}BF_3^+$. However, the 1790.4 cm^{-1} absorption might be contributed by a combination band involving the 1661.6 cm^{-1} absorption and a deformation vibration near 128 cm^{-1}, a remarkably low value.

To address these questions, new experiments were conducted on samples which were somewhat more concentrated in BF_3 than before, in order to enhance the intensities of product absorptions. Discharge sampling studies were conducted on samples in which not only BF_2OH but also its deuterium- and oxygen-18-containing isotopologs were present, in order

[a]Electronic mail: marilyn.jacox@nist.gov.
[b]Guest researcher.

to aid in identifying other products derived from BF_2OH. The results of these studies are presented in this paper.

II. EXPERIMENTAL DETAILS

The VLSI Grade BF_3 used in most of the earlier experiments was no longer available. Instead, a sample of BF_3 (Matheson Co., Inc.) (Ref. 7) was used without further purification. H_2O and samples of D_2O and $D_2{}^{18}O$ (Merck and Co./Isotopes) were frozen at 77 K, and the resulting solid was pumped on to remove traces of more volatile gases before being used for preparation of the mixture under study. Neon (Spectra Gases, Inc., Research Grade, 99.999%) was used without further purification.

Ne:BF_3 mixtures of mole ratio 400:1 were used for all but the earliest experiments, some of which were conducted on a Ne:BF_3 = 800:1 sample. Mixtures with Ne:BF_3:H_2O = 400:1:1 were prepared for the early studies, but the yield of BF_2OH was similar to that which appeared without added water. The optimum yield of either normal or isotopically enriched BF_2OH resulted when the deposition line was pretreated by establishing a slow flow of a Ne:H_2O = 400:1 mixture or of such a mixture made using D_2O or $D_2{}^{18}O$ through the system overnight or for a longer time period before starting the experiment. Hereafter, the mole ratios for such experiments will be expressed as 400:1:x, where x, the value for the water isotopolog, is not exactly known but is believed to be ~1. All mixtures containing BF_3 were prepared and handled in a vacuum manifold and deposition system constructed of Monel and stainless steel.

The sample mixtures were codeposited at 4.3 K with a similar amount of pure neon that had been excited by a microwave discharge before streaming through a 1 mm pinhole in the end of a quartz discharge tube. Details of the deposition procedure and of the discharge configuration have been described previously.[8,9] (The pure neon was not passed through a Nanochem filter in this series of experiments.)

The absorption spectra of the sample deposits were obtained using a Bomem DA 3.002 Fourier-transform interferometer with transfer optics that have been described previously.[10] All of the observations were conducted at a resolution of 0.2 cm^{-1} between 450 and 5000 cm^{-1} using a globar source, a KBr beamsplitter, and a wide-band HgCdTe detector cooled to 77 K. Data were accumulated for each spectrum over a period of at least 15 min. The resulting spectrum was ratioed against a similar one taken without a deposit on the cryogenic mirror. Under these conditions, the positions of the prominent, nonblended atmospheric water vapor lines between 1385 and 1900 cm^{-1} and between 3620 and 3900 cm^{-1}, observed in a calibration scan, agreed to within 0.01 cm^{-1} with the high resolution values reported by Toth.[11] Based on previous investigations, with this experimental configuration the standard uncertainty (type B) in the determination of the positions of the absorption maxima for molecules trapped in solid neon is ±0.1 cm^{-1} (coverage factor, $k = 1$, i.e., 1σ).

Information on photoinduced changes in the matrix sample was obtained by exposing the deposit to various wavelength ranges of near infrared, visible, and ultraviolet radiation. A tungsten background source was used with a filter of Schott glass type RG780 or RG695 to exclude radiation of wavelength shorter than ~780 or 695 nm, respectively. For irradiation at shorter wavelengths, a medium-pressure mercury arc source was used with a filter of Corning glass type 3384, 3389, 7380, or 7740 to exclude radiation of wavelength shorter than 490, 420, 345, or 280 nm, respectively. Some irradiations were also conducted using unfiltered medium-pressure mercury-arc radiation, estimated to have a cutoff wavelength near 240 nm.

TABLE I. Vibrational fundamentals (cm^{-1}) of BF_2OH.

		Medium	$^{11}BF_2OH$	$^{11}BF_2OD$
a′	ν_1	Ne matrix[a]	3712.5	2737.2
	ν_2	Ne matrix[a]	1464.3	1456.8
	ν_3	Ne matrix[a]	1414.9	1400.9
	ν_4	Gas phase[b,c]	961.49	
		Ne matrix[a]	959.1	879.3
	ν_5	Gas phase[c,d]	880.74	
		Ne matrix[a]	879.3	751.1
	ν_6	Gas phase[c,d]	479.17	
	ν_7	Gas phase[c,d]	446.54	
		Ne matrix[a]	447.5	481.5
a″	ν_8	Gas phase[b,d]	684.16	
		Ne matrix[a]	680.9	680.4
	ν_9	Gas phase[b,d]	522.87	
		Ne matrix[a]	520.8	

[a]Reference 5.
[b]Reference 6(a).
[c]Reference 6(b).
[d]Reference 6(c).
[e]Reference 6(d).

III. RESULTS AND DISCUSSION

A. Infrared survey

Prominent absorptions of BF_3 and of BF_2OH are present in all of the sample deposits. The positions of the BF_3 absorptions in a neon-matrix deposit were summarized in Table I of Ref. 5, and those of the BF_2OH and BF_2OD molecules trapped in solid neon and observed in the gas phase are summarized in Table I of this paper. The observations on BF_2 and $BF_2{}^+$ and the assignments for these products in the present study are similar to those previously reported.[1]

Moderately intense to strong, structured absorptions appeared near 500, 2080, and 2150 cm^{-1} in all of the discharge experiments. These are readily assigned to $F^{11}BO$ and $F^{10}BO$, previously identified in the neon-matrix experiments of Snelson.[12] The band center of the B = O stretching fundamental of gas-phase $F^{11}BO$ was found to lie at 2078.87 cm^{-1} in the high resolution diode laser study by Kawashima and co-workers.[13]

The positions and approximate relative intensities of the new absorptions which result on codeposition of a Ne:BF_3:H_2O sample with a beam of discharged Ne atoms are summarized in the first column of Table E-1.[14]

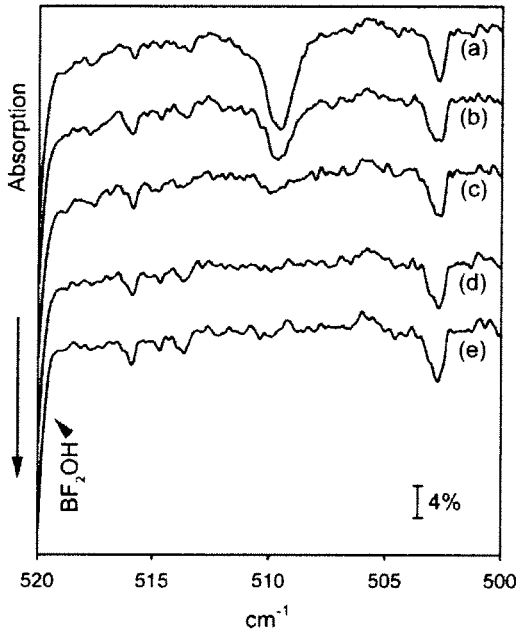

FIG. 1. Behavior of product absorptions between 500 and 520 cm^{-1} on sequential filtered mercury-arc irradiations. 13.4 mmol $Ne:BF_3:H_2O = 400:1:x$ codeposited at 4.3 K over a period of 230 min with 12.1 mmol pure neon that had been passed through a microwave discharge. (a) Initial deposit. (b) 20-min irradiation, $\lambda > 420$ nm (after previous irradiations with cutoff wavelength from 780 nm to 520 nm that resulted in little or no change in absorptions in this spectral region). (c) 20-min irradiation, $\lambda > 345$ nm. (d) 20-min irradiation, $\lambda > 280$ nm. (e) 20-min irradiation, unfiltered mercury arc.

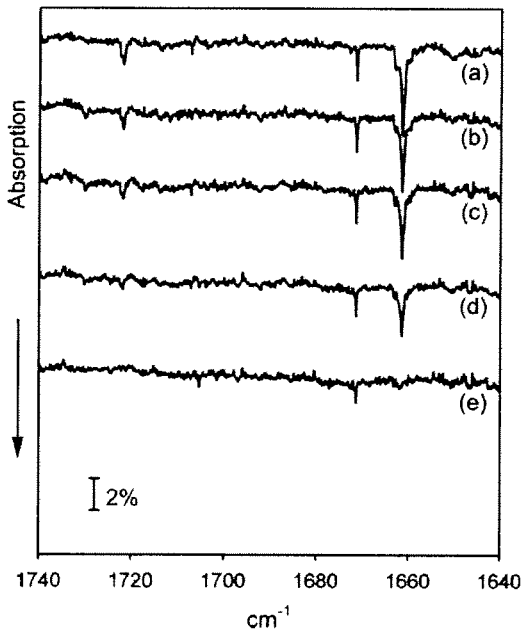

FIG. 2. Behavior of product absorptions between 1640 and 1740 cm^{-1} on sequential filtered mercury-arc irradiations. 13.4 mmol $Ne:BF_3:H_2O = 400:1:x$ codeposited at 4.3 K over a period of 230 min with 12.1 mmol pure neon that had been passed through a microwave discharge. (a) Initial deposit. (b) 20-min irradiation, $\lambda > 420$ nm (after previous irradiations with cutoff wavelength from 780 nm to 520 nm that resulted in little or no change in absorptions in this spectral region). (c) 20-min irradiation, $\lambda > 345$ nm. (d) 20-min irradiation, $\lambda > 280$ nm. (e) 20-min irradiation, unfiltered mercury arc.

B. Results of subsequent irradiation

The intensities of the prominent absorptions of BF_3 and BF_2OH grew somewhat as the sample was irradiated with visible and ultraviolet light, which releases electrons from various electron traps, making possible their capture by the cations of these two species to re-form the uncharged molecules. The behavior of the product absorptions when the discharge was used is summarized in the remaining columns of Table E-1.

The behavior on ultraviolet irradiation of major product absorptions that change little or not at all on visible irradiation of the deposit is shown in Figs. 1–4. (There had been previous filtered irradiations of the deposit before the one with a 420-nm cutoff that is shown as trace (b) in each of the figures. The cutoff wavelengths of these irradiations were at 780, 695, 630, and 520 nm.) Figure 4, for the 3230 to 3260 cm^{-1} spectral region, shows two new, weak to moderately intense absorptions which had been above the noise level in only one of the earlier experiments.[1]

The photodestruction behavior of several prominent product absorptions falls into two categories:

Category I. There is appreciable decrease in these absorptions when the 280-nm cutoff filter is used. The product absorptions of Fig. 2 (1661.6 and 1722.0 cm^{-1}) and of Fig. 4 (3240.1 and 3247.2 cm^{-1}) are in this category.

Category II. These peaks are appreciably reduced in intensity on irradiation through the 345-nm cutoff filter

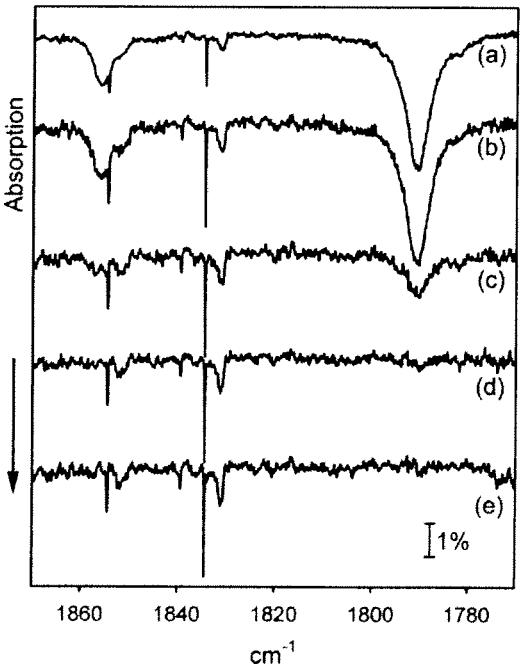

FIG. 3. Behavior of product absorptions between 1770 and 1870 cm^{-1} on sequential filtered mercury-arc irradiations. 13.4 mmol $Ne:BF_3:H_2O = 400:1:x$ codeposited at 4.3 K over a period of 230 min with 12.1 mmol pure neon that had been passed through a microwave discharge. (a) Initial deposit. (b) 20-min irradiation, $\lambda > 420$ nm (after previous irradiations with cutoff wavelength from 780 nm to 520 nm that resulted in little or no change in absorptions in this spectral region). (c) 20-min irradiation, $\lambda > 345$ nm. (d) 20-min irradiation, $\lambda > 280$ nm. (e) 20-min irradiation, unfiltered mercury arc.

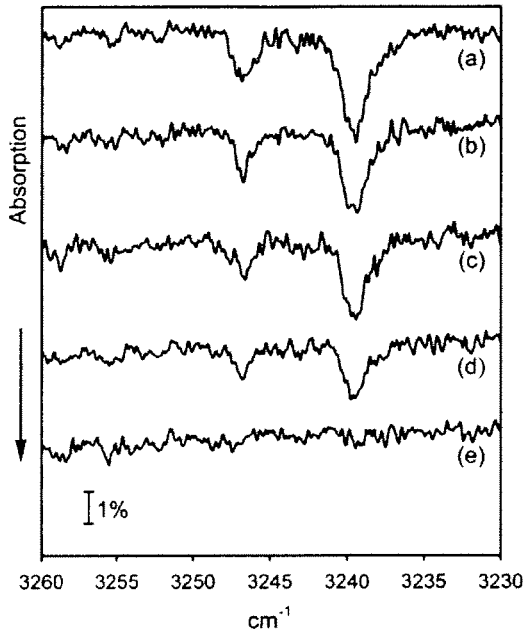

FIG. 4. Behavior of product absorptions between 3230 and 3260 cm^{-1} on sequential filtered mercury-arc irradiations. 13.4 mmol $Ne:BF_3:H_2O = 400:1:x$ codeposited at 4.3 K over a period of 230 min with 12.1 mmol pure neon that had been passed through a microwave discharge. (a) Initial deposit. (b) 20-min irradiation, $\lambda > 420$ nm (after previous irradiations with cutoff wavelength from 780 nm to 520 nm that resulted in little or no change in absorptions in this spectral region). (c) 20-min irradiation, $\lambda > 345$ nm. (d) 20-min irradiation, $\lambda > 280$ nm. (e) 20-min irradiation, unfiltered mercury arc.

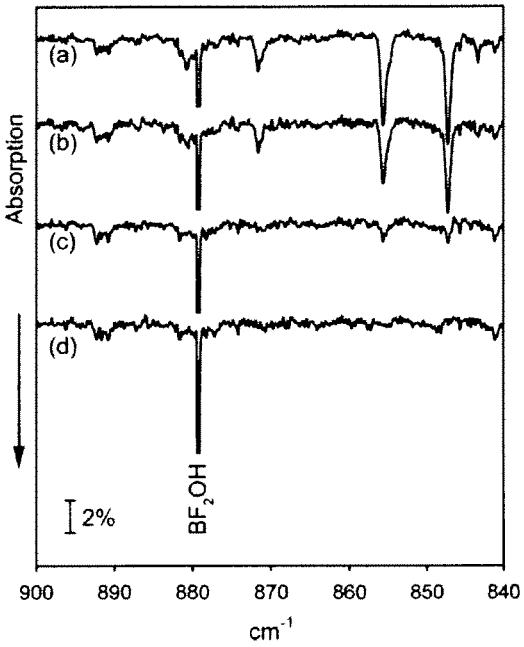

FIG. 5. Behavior of product absorptions between 840 and 900 cm^{-1} on sequential filtered tungsten-lamp irradiations. 13.4 mmol $Ne:BF_3:H_2O = 400:1:x$ codeposited at 4.3 K over a period of 230 min with 12.1 mmol pure neon that had been passed through a microwave discharge. (a) Initial deposit. (b) 20-min irradiation, $\lambda > 780$ nm. (c) 20-min irradiation, $\lambda > 695$ nm. (d) 20-min irradiation, $\lambda > 630$ nm.

and are almost completely destroyed by radiation of wavelength between 345 and 280 nm. This behavior pattern is shown by the product absorptions of Fig. 1 (509.6 cm^{-1}) and of Fig. 3 (1790.8 and 1856.4 cm^{-1}).

The absorptions of FBO (at 496.7, 2077.3, and 2150.4 cm^{-1}), which continue to grow in intensity throughout the irradiation sequence, those of BF_2 (at 523.8, 529.4, 1151.5, 1181.6, 2534.0, and 2612.3 cm^{-1}) and BF_2^+ (at 2026.0 and 2101.4 cm^{-1}), and the absorptions at 823.3, 830.4, and 1059.1 cm^{-1}, do not fit into these two categories.

As is shown in Figs. 5 and 6, other absorptions are destroyed by visible radiation. Peaks at 594.4, 595.2, 847.2, 855.7, 871.7, 880.7, 1001.8, 1002.2, 1004.7, 1021.7, 1026.4, 1056.2, and 1061.4 cm^{-1} decrease slightly in intensity on 780-nm cutoff tungsten-lamp irradiation and are almost destroyed when that filter is replaced by one with a 695-nm cutoff.

C. Behavior in experiments using D_2O and $D_2{}^{18}O$

The positions of the product absorptions summarized in Table E-1 are compared with their counterparts in experiments using isotopically substituted water in Table E-2.[14] Many of these product absorptions are contributed by normal and isotopically substituted BF_2OH. Their assignments have previously been given,[5] and are summarized in Table E-2. Only a few of the remaining absorptions shift on isotopic

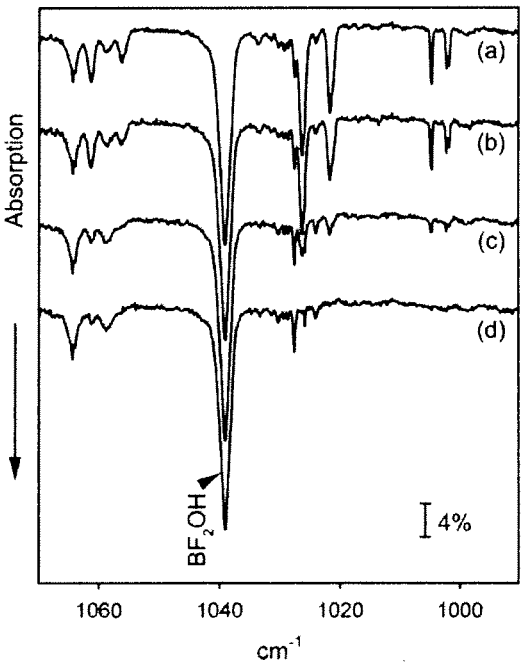

FIG. 6. Behavior of product absorptions between 990 and 1070 cm^{-1} on sequential filtered tungsten-lamp irradiations. 13.4 mmol $Ne:BF_3:H_2O = 400:1:x$ codeposited at 4.3 K over a period of 230 min with 12.1 mmol pure neon that had been passed through a microwave discharge. (a) Initial deposit. (b) 20-min irradiation, $\lambda > 780$ nm. (c) 20-min irradiation, $\lambda > 695$ nm. (d) 20-min irradiation, $\lambda > 630$ nm.

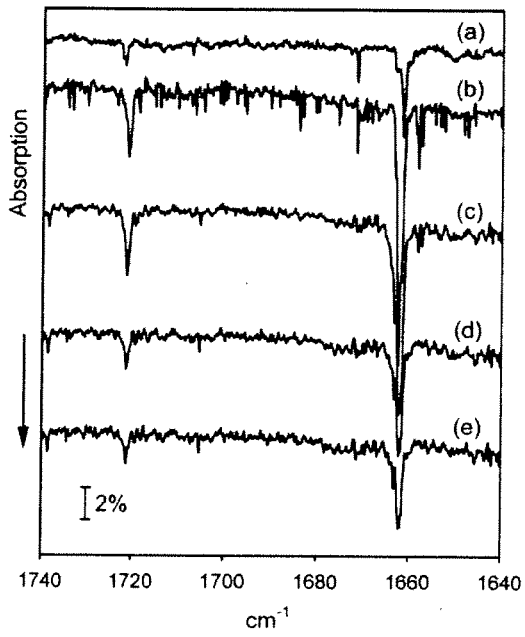

FIG. 7. Behavior of product absorptions between 1640 and 1740 cm^{-1} on enrichment of $Ne:BF_3:H_2O$ samples in deuterium and in oxygen-18. (a)13.4 mmol $Ne:BF_3:H_2O$ = 400:1:x codeposited at 4.3 K over a period of 230 min with 12.1 mmol pure neon that had been passed through a microwave discharge. (b) 16.0 mmol $Ne:BF_3:D_2O$ = 400:1:x codeposited at 4.3 K over a period of 277 min with 14.1 mmol pure neon that had been passed through a microwave discharge. (c) 13.8 mmol $Ne:BF_3:D_2{}^{18}O$ = 400:1:x codeposited at 4.3 K over a period of 240 min with 12.3 mmol pure neon that had been passed through a microwave discharge. (d) Deposit (c), after 20-min mercury-arc irradiation, $\lambda > 345$ nm. (e) Deposit (d), after 20-min mercury-arc irradiation, $\lambda > 280$ nm.

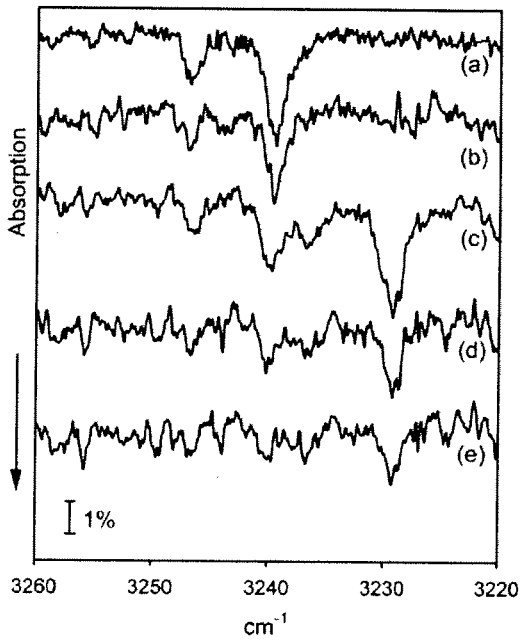

FIG. 8. Behavior of product absorptions between 3220 and 3260 cm^{-1} on enrichment of $Ne:BF_3:H_2O$ samples in deuterium and in oxygen-18. (a) 13.4 mmol $Ne:BF_3:H_2O$ = 400:1:x codeposited at 4.3 K over a period of 230 min with 12.1 mmol pure neon that had been passed through a microwave discharge. (b) 16.0 mmol $Ne:BF_3:D_2O$ = 400:1:x codeposited at 4.3 K over a period of 277 min with 14.1 mmol pure neon that had been passed through a microwave discharge. (c) 13.8 mmol $Ne:BF_3:D_2{}^{18}O$ = 400:1:x codeposited at 4.3 K over a period of 240 min with 12.3 mmol pure neon that had been passed through a microwave discharge. (d) Deposit (c), after 20-min mercury-arc irradiation, $\lambda > 345$ nm. (e) Deposit (d), after 20-min mercury-arc irradiation, $\lambda > 280$ nm.

substitution. One of these is FBO; the assignments for $FB^{18}O$ are straightforward, and are included in Table E-2. Three other unassigned absorptions, all of which are insensitive on exposure of the deposit to visible light but are destroyed on mercury-arc irradiation of the deposit with a 280-nm cutoff filter, will be considered in this section.

Figure 7 compares the 1640 to 1740 cm^{-1} spectral region for all three isotopologs of H_2O that were studied in these experiments. The major absorption, at 1661.6 cm^{-1}, shows some partially resolved structure which can be attributed to the trapping of its carrier in multiple sites in the neon solid. As in the earlier study,[1] its counterpart containing boron-10 contributes a much weaker absorption at 1722.0 cm^{-1}. The spectra of Fig. 7 show no evidence of new peaks when either $D_2{}^{16}O$ or $D_2{}^{18}O$ is present in the sample. An ~0.5 cm^{-1} upward shift in the 1661.6 cm^{-1} absorption consistently occurs when D_2O is used, and there is neither any lower frequency counterpart nor any further shift when $D_2{}^{18}O$ is used instead of $D_2{}^{16}O$. The photodestruction properties noted in the preceding paragraph are illustrated for $D_2{}^{18}O$ substitution in traces (c), (d), and (e).

Trace (a) of Fig. 8 shows a peak at 3240.1 cm^{-1} with a higher frequency satellite at 3247.2 cm^{-1}, a spectral region appropriate for an OH-stretching vibration. These two peaks, like that at 1661.6 cm^{-1}, were destroyed by mercury-arc radiation passed by a 280-nm cutoff filter. As is shown in traces (b) and (c), they persisted in experiments on sample mixtures containing $D_2{}^{16}O$ and $D_2{}^{18}O$; full isotopic enrichment of water is difficult to achieve. However, when–as in trace (c)–^{18}O is present in the water, a new pair of absorptions with the same photodestruction behavior appears at 3229.1 and 3236.8 cm^{-1}. The magnitude of the shift is consistent with the assignment of this pair of product absorptions to an OH-stretching vibration, split by the trapping of their carrier in two different sites in solid neon.

Trace (a) of Fig. 9 shows the absorption pattern observed between 2380 and 2410 cm^{-1} in the high-yield $Ne:BF_3:D_2O$ = 400:1:x experiment for which other spectral regions are shown in Figs. 7(b) and 8(b). New absorptions appeared at 2395.7 and 2401.3 cm^{-1}. As is shown in the remaining traces of Fig. 9, the photodestruction behavior of these two absorptions is similar to that of the absorptions near 1662, 1722, 3240, and 3247 cm^{-1} that have previously been discussed. The ratios of the 2395.7 cm^{-1} absorption frequency to that at 3240.1 cm^{-1} and of the 2401.3 cm^{-1} absorption frequency to that at 3247.2 cm^{-1} both equal 0.739, appropriate for the assignment of the pair of absorptions shown in Fig. 9 to an OD-stretching vibration. The position of the corresponding absorption of the product containing oxygen-18 is uncertain.

Analysis of the isotopic substitution observations was facilitated by calculations of the isotopic substitution behavior of the vibrational fundamentals of BF_2O and of ionic species

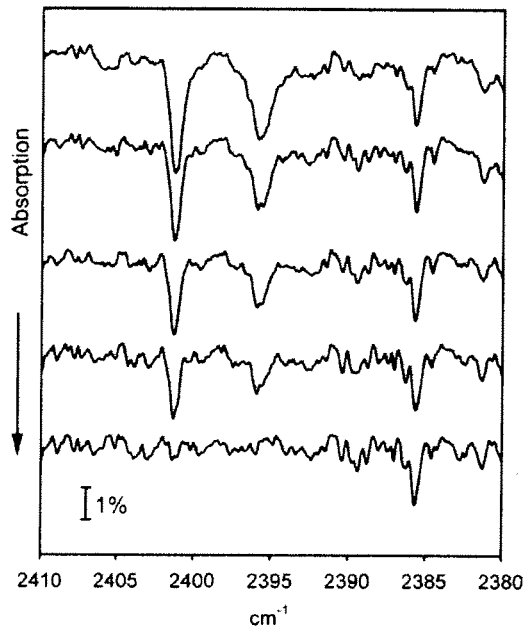

FIG. 9. Behavior of product absorptions between 2380 and 2410 cm^{-1} on sequential filtered mercury-arc irradiations. 16.0 mmol Ne:BF_3:$D_2{}^{16}O$ = 400:1:x codeposited at 4.3 K over a period of 277 min with 14.1 mmol pure neon that had been passed through a microwave discharge. (a) Initial deposit. (b) 20-min irradiation, $\lambda > 420$ nm. (c) 20-min irradiation, $\lambda > 345$ nm. (d) 20-min irradiation, $\lambda > 280$ nm. (e) 20-min irradiation, unfiltered mercury arc.

of formula BF_nO and BF_nOH (n = 0, 1) using the GAUSSIAN 03 program package.[15] The positions of the ground-state fundamentals were obtained by density functional calculations using the unrestricted B3LYP procedure[16] together with the correlation-consistent polarized valence triple-zeta basis set (cc-pVTZ) developed by Dunning.[17] In some of the calculations, the basis set was augmented by the inclusion of diffuse functions.

D. Infrared spectrum of BF_2OH^+

The prominence of the absorptions of BF_2OH in the present experiment and–as already noted–the appearance of oxygen-containing cations in the spectra of other fluorides suggest that absorptions of BF_2OH^+ may contribute to the observed spectrum. The results of the density functional calculations for normal and isotopically substituted BF_2OH^+ are summarized and suitable assignments are proposed in Table II. The most prominent absorptions of the unenriched species lie near 3450 and 1625 cm^{-1}. The disparity of $\sim$ 200 cm^{-1} between the calculated OH stretching absorption of BF_2OH^+ and the absorption observed at 3240.1 cm^{-1} may result from a combination of the anharmonic correction ($\sim$100 cm^{-1}) and a shift to lower wavenumbers because of proton sharing by BF_2OH^+ with the neon matrix.[18] The calculated $^{11}BF_2$ antisymmetric stretching fundamental at 1624.2 cm^{-1} lies sufficiently close to the observed absorption at 1661.6 cm^{-1} to support reassignment of that peak to the $^{11}BF_2$ antisymmetric stretching fundamental of BF_2OH^+. The calculated frequency shift for that fundamental of $^{10}BF_2OH^+$ is also consistent with the appearance of that absorption at 1722.0 cm^{-1}. Those two absorptions are both calculated and observed to shift by less than 1 cm^{-1} on oxygen-18 or deuterium substitution, consistent with the proposed assignment.

E. Infrared spectrum of BF_3^+

Comparison of the spectroscopic properties of BF_3^+ with those of the important atmospheric reaction intermediate NO_3 is key to understanding the spectra of both molecules. Both species possess 23 valence electrons and, in the first approximation, would be expected to have planar, threefold-symmetric (D_{3h}) ground-state structures, with two vibrational fundamentals of e′ symmetry. Both species possess two low-lying excited electronic states at quite similar energies, and the electronic symmetries of these states match. Each molecule has a $^2A_2'$ ground state, whereas the next higher electronic states have $^2E''$ and $^2E'$ symmetry, respectively. Not only can each of these excited states exhibit Jahn-Teller distortion, but also vibronic interaction of the $^2E'$ excited electronic state with the two ground-state fundamentals of e′ symmetry (*pseudo*-Jahn-Teller interaction) may have a profound influence on the structure and spectrum of the ground-state molecule. The same theory has been applied to both systems,

TABLE II. Vibrational fundamentals (cm^{-1}) of BF_2OH^+.

			$F_2{}^{11}B^{16}OH^+$	$F_2{}^{10}B^{16}OH^+$	$F_2{}^{11}B^{18}OH^+$	$F_2{}^{11}B^{16}OD^+$	$F_2{}^{11}B^{18}OD^+$
a′	ν_1	Calculated[a]	3448.6(422)	3448.6(422)	3437.2(422)	2511.2(208)	2495.3(209)
		Observed[b]	3240.1	3240.1	3229.1	2395.7	
	ν_2	Calculated [a]	1134.9(78)	1160.9(90)	1134.8(78)	1134.5(85)	1134.4(85)
	ν_3	Calculated [a]	839.1(179)	847.8(183)	834.7(180)	704.2(107)	698.9(103)
	ν_4	Calculated [a]	688.5(25)	698.3(25)	673.9(30)	685.6(16)	672.3(27)
	ν_5	Calculated [a]	518.7(66)	534.0(72)	518.4(68)	459.3(27)	456.6(35)
	ν_6	Calculated [a]	431.1(41)	432.5(41)	422.2(35)	424.2(64)	417.2(52)
a″	ν_7	Calculated [a]	1624.2(264)	1681.8(287)	1624.2(264)	1623.9(257)	1623.9(257)
		Observed [b]	1661.6	1722.0	1662.1	1662.3	1662.1
	ν_8	Calculated [a]	375.1(130)	375.4(130)	369.4(136)	320.5(44)	312.6(47)
	ν_9	Calculated [a]	208.8(35)	209.7(35)	206.6(31)	178.5(32)	178.1(30)

[a]UB3LYP/cc-pVTZ calculations. Intensities (km/mol) are given in parentheses.

[b]This work. Based on previous investigations, the standard uncertainty (type B) in the neon-matrix measurements is 0.1 cm^{-1} (1σ).

but has been elaborated in greater detail for NO_3 than for BF_3^+, making this comparison particularly useful.

Haller and co-workers[19] developed the basic theory for interpreting the photoelectron spectra of molecules for which such vibronic interactions occur and found it to predict a C_{2v} structure for ground-state BF_3^+. In a preliminary note, Haller and co-workers[20] had successfully predicted the occurrence and magnitude of the *pseudo*-Jahn-Teller effect in higher energy photoelectron bands of BF_3^+. Their calculations showed that, as a result of interaction of the $\tilde{E}^2A_1'$ state of BF_3^+ with a nearby $^2E'$ electronic state, single quanta of the degenerate stretching vibration were excited in the photoelectron spectrum of the $\tilde{E}$ state.

Haller and co-workers[19] found that the two e′ fundamentals of ground-state BF_3^+, ν_3 and ν_4, should be strongly coupled and that their *pseudo*-Jahn-Teller interaction with the $\tilde{B}^2E'$ excited electronic state should be strong. The barrier separating the resulting C_{2v} structure from the D_{3h} one amounts to 0.042 eV.

Similar calculations by the Köppel group for NO_3 (Ref. 21) indicate that ground-state NO_3 behaves quite differently from BF_3^+. The barrier height for the C_{2v} minimum (with one short and two long NO bonds) of NO_3 with respect to the D_{3h} structure is only 0.006 eV, so that effectively NO_3 remains threefold symmetric. Experiments and later calculations support the D_{3h} structure. Stanton[22,23] extended the earlier calculations by Mayer and co-workers[21] to predict the vibrational energy levels of ground-state NO_3, for which many anomalies had been attributed to substantial interaction between ground-state vibrations of e′ symmetry and the $\tilde{B}^2E'$ electronic state, for which the origin lies near 15100 cm^{-1}. These calculations indicated that the ν_3 fundamental of NO_3 should be exceptionally weak and should lie in the 1000–1100 cm^{-1} spectral region. As yet, such an absorption has not been detected. In general, there is good agreement of the calculated energy level pattern with the gas-phase observations below ~2500 cm^{-1}. Neon-matrix observations by Jacox and Thompson[24] of the infrared spectra of eight isotopologs of NO_3 also agree well with the gas-phase band centers. Moreover, the observed isotopic shifts for the species which retain D_{3h} symmetry agree very well with those calculated by Stanton.[23]

The first photoelectron band of BF_3 is very broad. Some studies show hints of vibrational structure, not yet definitively assigned. Yencha and co-workers[25] identified two partially resolved, overlapping progressions with average spacings of 411(32) cm^{-1} and 202(24) cm^{-1} in the first band of the threshold photoelectron spectrum of BF_3. By analogy with the assignments proposed in our earlier paper,[1] they suggested the assignment of these two progressions to bands involving ν_4 and ν_2, respectively, of ground-state BF_3^+. However, subsequent observations by Mackie and co-workers[26] did not reproduce these two vibrational progressions. Weaver and co-workers[27] noted progressions involving a single quantum of ν_4 in the photoelectron band of NO_3^- which they assigned to ground-state NO_3. The calculations by Mayer and co-workers[21] confirm this behavior for ν_4 of ground-state NO_3 and imply that it is likely also to occur for ν_4 of ground-state BF_3^+. As already noted, excitation of a single quantum of an e′ vibration was also observed in the photoelectron band of the $\tilde{E}^2A_1'$ state of BF_3^+ and was explained by application of the same basic theory.[20] Within the experimental uncertainty, the spacings attributed by Yencha and co-workers to progressions in the deformation fundamentals of BF_3^+ differ by a factor of two. If single quanta of the degenerate bending fundamental of ground-state BF_3^+ are detectable in the photoelectron spectrum, the two progressions would merge into one progression with vibrational separations of ~202 cm^{-1}, contributed by ν_4 of ground-state BF_3^+.

The calculations suggest that the out-of-plane deformation fundamental, ν_2, of NO_3 and that of BF_3^+ in their ground states are relatively unaffected by the interaction of the three lowest electronic states of those molecules. The gas-phase studies and the isotopic shifts observed in the neon-matrix study of NO_3 support this generalization. The assignment of the relatively broad 509.6 cm^{-1} absorption with Category II photodestruction behavior in the present study to that fundamental of BF_3^+ would also be consistent with it.

The present studies support the previous assignment[1] of the broad absorption at 1790.8 cm^{-1} to $^{11}BF_3^+$ and of its less intense counterpart at 1856.4 cm^{-1} to $^{10}BF_3^+$. The relatively great breadth of these two absorptions, as well as of the remaining Category II absorption at 509.6 cm^{-1}, is reminiscent of the broadness of the first photoelectron band of BF_3^+, which in the gas phase readily photodissociates into $BF_2^+ + F$. The boron-isotopic shift would be appropriate for either ν_3 or $2\nu_3$. However, the calculations by Haller and co-workers[19] favor the assignment of the two high-frequency absorptions to the ν_3 fundamental of the two isotopologs of BF_3^+, distorted by *pseudo*-Jahn-Teller interaction. These calculations indicate that one BF bond is lengthened by 0.11 Å and each of the other two BF bonds are shortened by ~0.055 Å. The valence angle between these two short BF bonds opens out by 24° to 144°. The resulting structure approaches that for BF_2^+ in a weakly bound complex with the remaining F atom. The calculations by Atkinson and co-workers[28] indicate that the ionization of BF_2 to BF_2^+ shortens the two BF bond lengths from 1.32 Å to 1.23 Å and increases the FBF valence angle from 121.3° to 180°. The calculated position for ν_3 of $^{11}BF_2^+$ is 2055 cm^{-1}. The earlier experiments in this laboratory[1] are consistent with these predictions. Whereas the ν_3 fundamental of $^{11}BF_2$ trapped in solid neon appeared at 1442.4 cm^{-1}, that of $^{11}BF_2^+$ was raised to 2026.1 cm^{-1}. By analogy, the calculations of Haller and co-workers suggest that ν_3 of $^{11}BF_3^+$ should be shifted to an appreciably higher frequency than the 1450-cm^{-1} value for the uncharged species.

The assignments here proposed for the vibrational fundamentals of ground-state $^{11}BF_3^+$ are summarized in Table III. The boron-10 counterpart of the 1790.8 cm^{-1} absorption of $^{11}BF_3^+$ is observed (see Fig. 3) at 1856.4 cm^{-1}. As in the earlier study,[1] the peak at 509.6 cm^{-1} is attributed to BF_3^+. Because this absorption is near the low-frequency edge of the beamsplitter response and because there are several nearby strong absorptions of other species, the boron-10 counterpart of the 509.6 cm^{-1} peak has not been de-

TABLE III. Vibrational fundamentals (cm^{-1}) of $^{11}BF_3^+$.

Symmetry	Vibration	Type of mode	cm^{-1}	Medium
a_2''	ν_2	Out-of-plane deformation	509.6	Ne matrix[a]
e'	ν_3	BF_3 stretch	1790.8	Ne matrix[a]
	ν_4	Deformation	202(24)	Gas phase[b]

[a]Reference 1; this work. Based on previous investigations, the standard uncertainty (type B) in the neon-matrix measurements is 0.1 cm^{-1} (1σ).
[b]Reference 25.

tected. The possible contribution by single quanta of ν_4 of the ground-state cation of the 202(24) cm^{-1} progression reported in one study[25] of the first band in the photoelectron spectrum of BF_3 has already been noted. Assignment of the 509.6 cm^{-1} peak to ν_2 of BF_3^+ is suggested.

F. Infrared spectra of other products

Although BF_2OH^- might be predicted to be a likely product, calculations for that species gave one imaginary vibrational frequency, suggesting that it does not possess a stable potential minimum.

Several absorptions, all below 1100 cm^{-1}, are distinguished by the ease with which they are destroyed on exposure of the deposit to visible radiation. The photodestruction behavior summarized in Table E-1[14] for these absorptions is approximate; often the detection limits for the weaker absorptions occur at somewhat higher frequencies, or shorter wavelengths, than those for their more intense counterparts. None of these absorptions shift in frequency in the presence of isotopically labelled water. As previously noted,[1] their positions are appropriate for BF-stretching modes of BF_n^- species. More recent studies are helpful in considering their assignments.

Because the concentration of BF_3 in the deposit is considerably greater than that of any of the product molecules, electron capture by BF_3 may be an important process. Hudson and co-workers[29] recorded the electron spin resonance spectrum of BF_3^- trapped in solid tetramethylsilane. Like CF_3, with which it is isoelectronic, BF_3^- was found to be pyramidal, with a C_{3v} structure. Calculations by Gutsev and co-workers[30] found a value of −0.76 eV for the adiabatic electron affinity of BF_3. However, at the equilibrium geometry of BF_3, the total energy of the neutral is 0.95 eV higher than that of BF_3^-. The harmonic fundamental frequencies which these workers obtained for BF_3^- are summarized in Table IV, as are those recently obtained by Grant and co-workers.[31] The latter study obtained a value of −0.56 eV for the adiabatic electron affinity of BF_3 using the CCSD(T) procedure and the complete basis set. The values obtained for the fundamental frequencies in all of the calculations are consistent. Moreover, they support the identification of two vibrational fundamentals and one combination band of $^{11}BF_3^-$ in the present neon-matrix study, proposed in Table IV. The doubling of each of the three observed absorptions probably results from trapping of BF_3^- in two or more different sites in solid neon. The ν_3 vibrational fundamental and the $\nu_2 + \nu_4$ combination band, both of e symmetry, are sufficiently close to make Fermi resonance interaction between those two energy levels probable.

TABLE IV. Energy levels of ground-state $^{11}BF_3^-$ (C_{3v}).

Energy Level	Method/Medium	cm^{-1}
ν_4 (e)	MBPT(4)/6–311+G(2d) [a]	414
	CCSD(T)/6–311+G(2d) [a]	417
	MP2/aug-cc-pVTZ [b]	411.3
ν_2 (a_1)	MBPT(4)/6–311+G(2d) [a]	591
	CCSD(T)/6–311+G(2d) [a]	594
	MP2/aug-cc-pVTZ [b]	574.6
	Ne matrix [c]	594.4, 595.2
ν_1 (a_1)	MBPT(4)/6–311+G(2d) [a]	760
	CCSD(T)/6–311+G(2d) [a]	776
	MP2/aug-cc-pVTZ [b]	741.1
$\nu_2 + \nu_4$ (e)	MBPT(4)/6–311+G(2d) [a,d]	1005
	CCSD(T)/6–311+G(2d) [a,d]	1011
	MP2/aug-cc-pVTZ [b,d]	985.9
	Ne matrix [c]	1002.2, 1004.7
ν_3 (e)	MBPT(4)/6–311+G(2d) [a]	1051
	CCSD(T)/6–311+G(2d) [a]	1064
	MP2/aug-cc-pVTZ [b]	1078.4
	Ne matrix [c]	1021.7, 1026.4

[a]Reference 30.
[b]Reference 31.
[c]This work. Based on previous investigations, the standard uncertainty (type B) in the neon-matrix measurements is 0.1 cm^{-1} (1σ).
[d]Sum of ν_2 and ν_4.

QCISD(T)/6–311+G* calculations by Atkinson and co-workers[28] yielded an adiabatic electron affinity of 1.14 eV for BF_2 and a vertical detachment energy of 1.64 eV for BF_2^-. Their B3LYP calculations using the same basis set yielded values that are ~0.15 eV smaller. Their calculated positions for the harmonic vibrational fundamentals of $^{11}BF_2^-$ and $^{10}BF_2^-$ are summarized in Table V, together with our proposed assignments for the remaining relatively low frequency absorptions in the present neon-matrix studies. Although the observed absorptions each lie about 70 cm^{-1} below the calculated values, that disparity may result in part from the comparison of calculated harmonic values with observed anharmonic ones.

Another possible product in these experiments, BF_4^-, has been the subject of several experimental and theoretical studies. Greenwood[32] observed the infrared spectra of crystalline KBF_4 (presumed to be highly ionic) and of that material enriched to 90% in boron-10 both in Nujol mulls and in KBr

TABLE V. Vibrational fundamentals (cm^{-1}) of BF_2^-.

Vibration	Method/medium	$^{11}BF_2^-$	$^{10}BF_2^-$
ν_1 (a_1)	QCISD(T)/6–311+G* [a]	914	942
	Ne matrix[b]	847.2	871.7
ν_2 (a_1)	QCISD(T)/6–311+G* [a]	515	519
ν_3 (b_2)	QCISD(T)/6–311+G* [a]	922	953
	Ne matrix[b]	855.7	880.7

[a]Reference 28.
[b]This work. Based on previous investigations, the standard uncertainty (type B) in the neon-matrix measurements is 0.1 cm^{-1} (1σ).

disks. The absorption maximum of ν_4 of $K^{11}BF_4$ appeared at 530 cm^{-1} and that of $K^{10}BF_4$ at 542 cm^{-1}. However, the infrared spectrum in the expected region of the BF-stretching vibrations was very complicated. For unenriched KBF_4, six very prominent absorption maxima appeared between 1032 and 1128 cm^{-1}. Because $2\nu_4$ of KBF_4 lies close to ν_3, Greenwood suggested that the F_2 component of $2\nu_4$ might be in Fermi resonance with ν_3. The computational study by Gutsev and co-workers[30] found that uncharged BF_4 is a van der Waals complex, with the fourth F atom out of the plane of the BF_3 moiety and with a binding energy of 1.6 kcal/mol (6.7 kJ/mol). In contrast, BF_4^- has tetrahedral symmetry and is stable by 3.58 eV with respect to F^- detachment. Their MBPT(4)/6–311G(2d) calculations obtained positions of 513 and 1067 cm^{-1} for the two fundamentals of BF_4^- with f_2 symmetry. The corresponding CCSD(T)/6–311G(2d) calculations yielded positions of 518 and 1082 cm^{-1} for these two fundamentals of BF_4^-. The recent calculations by Grant and co-workers[31] at the MP2/aug-cc-pVTZ level yielded similar vibrational frequencies for BF_4^-. These workers obtained a fluoride affinity of 81.1 kcal/mol (339 kJ/mol) for BF_3 at 0 K, corresponding to a stability of BF_4^- with respect to F^- detachment of 3.52 eV. Thus, both of these computational studies imply that the BF_4^- absorptions in our experiments should be quite photostable and, if F^- can diffuse through the matrix, might even grow in intensity during the course of all or most of the filtered irradiations. An infrared absorption at 1064.4 cm^{-1} fits these criteria and is tentatively assigned to BF_4^-.

It has previously been proposed[1] that three broad absorptions between 545 and 560 cm^{-1} which grow in intensity throughout the course of subsequent irradiations of the deposit may be contributed by ν_3 of F_3^-. These absorptions also appear in the present experiments and behave in a similar manner on irradiation. However, a recent paper by Riedel and co-workers[33] has proposed an alternate assignment of an absorption at 524.7 cm^{-1} to the antisymmetric stretching fundamental of F_3^- isolated in a neon matrix. Another possible assignment of the three absorptions between 545 and 560 cm^{-1} might be to the lower frequency infrared-active fundamental of BF_4^-. The assignment of these absorptions remains uncertain.

IV. CONCLUSIONS

The OH stretching and BF_2 antisymmetric stretching fundamentals of BF_2OH^+ have been identified for the first time. The previously proposed assignment of two of the vibrational fundamentals of BF_3^+ is supported by these new studies. The boron-isotopic shift in the position of the 1790.8 cm^{-1} absorption is appropriate for its assignment to the degenerate stretching fundamental, ν_3, of BF_3^+. The unusually high frequency observed for this fundamental is consistent with the calculated C_{2v} structure for ground-state BF_3^+, taking into account the *pseudo*-Jahn-Teller coupling between the $\tilde{B}^2E'$ and $\tilde{X}^2A_2'$ states of BF_3^+. Assignments proposed for several of the infrared absorptions of BF_3^- and of BF_2^- are consistent with the results of high level *ab initio* calculations.

ACKNOWLEDGMENTS

The authors wish to thank Dr. Lester Andrews, of the University of Virginia, Charlottesville, for the sample of BF_3 used in these experiments.

[1] M. E. Jacox and W. E. Thompson, J. Chem. Phys. **102**, 4747 (1995).
[2] C. L. Lugez, K. K. Irikura, and M. E. Jacox, J. Chem. Phys. **108**, 8381 (1998).
[3] C. L. Lugez, M. E. Jacox, R. A. King, and H. F. Schaefer III, J. Chem. Phys. **108**, 9639 (1998).
[4] H.Takeo and R. F. Curl, J. Chem. Phys. **56**, 4314 (1972).
[5] M. E. Jacox, K. K. Irikura, and W. E. Thompson, J. Chem. Phys. **113**, 5705 (2000).
[6] (a) D. Collet, A. Perrin, H. Bürger, and J.-M. Flaud, J. Mol. Spectrosc. **212**, 118 (2002); (b) J. Breidung, J. Demaison, J.-F. D'Eu, L. Margulès, D. Collet, E. B. Mkadmi, A. Perrin, and W. Thiel, *ibid.* **228**, 7 (2004); (c) A. Perrin, M. Carvajal-Zaera, Z. Dutkiewicz, J.-M. Flaud, D. Collet, H. Bürger, J. Demaison, F. Willaert, H. Mäder, and N. W. Larsen, Mol. Phys. **102**(14–15), 1641 (2004); (d) A. Perrin, E. Bertseva, J.-M. Flaud, D. Collet, H. Bürger, T. Massiello, and T. A. Blake, *ibid.* **105**(13–14), 1833 (2007).
[7] Certain commercial instruments and materials are identified in this paper in order to specify adequately the experimental procedure. In no case does such identification imply recommendation or endorsement by the National Institute of Standards and Technology, nor does it imply that the instruments or materials identified are necessarily the best available for the purpose.
[8] M. E. Jacox and W. E. Thompson, J. Chem. Phys. **91**, 1410 (1989).
[9] D. Forney, W. E. Thompson, and M. E. Jacox, J. Chem. Phys. **97**, 1664 (1992).
[10] M. E. Jacox and W. B. Olson, J. Chem. Phys. **86**, 3134 (1987).
[11] R. A. Toth, J. Opt. Soc. Am. B **8**, 2236 (1991); *ibid.***10**, 2006 (1993).
[12] A. Snelson, High Temp. Sci. **4**, 141 (1972).
[13] Y. Kawashima, K. Kawaguchi, Y. Endo, and E. Hirota, J. Chem. Phys. **87**, 2006 (1987).
[14] See supplementary material at http://dx.doi.org/10.1063/1.3587133 for Tables E-1 and E-2, concerned with the positions, intensities, and behavior on subsequent irradiation of the new absorptions which result on codeposition at 4.3 K of a normal or an isotopically enriched mixture of boron trifluoride and water in a large excess of neon with a beam of neon atoms that had been excited in a microwave discharge.
[15] M. J. Frisch, G. W. Trucks, H. B. Schlegel *et al.* GAUSSIAN 03, Revision B.01, Gaussian, Inc., Wallingford, CT, 2004).
[16] A. D. Becke, J. Chem. Phys. **98**, 5648 (1993); C. Lee, W. Yang, and R. G. Parr, Phys. Rev. B **37**, 785 (1988).
[17] T. H. Dunning, J. Chem. Phys. **90**, 1007 (1989).
[18] E. J. Bieske and O. Dopfer, Chem. Rev. **100**, 3963 (2000).
[19] E. Haller, H. Köppel, L. S. Cederbaum, W. von Niessen, and G. Bieri, J. Chem. Phys. **78**, 1359 (1983).
[20] E. Haller, H. Köppel, L. S. Cederbaum, G. Bieri, and W. von Niessen, Chem. Phys. Lett. **85**, 12 (1982).
[21] M. Mayer, L. S. Cederbaum, and H. Köppel, J. Chem. Phys. **100**, 899 (1994).
[22] J. F. Stanton, J. Chem. Phys. **126**, 134309 (2007).
[23] J. F. Stanton, Mol. Phys. **107**, 1059 (2009).
[24] M. E. Jacox and W. E. Thompson, J. Chem. Phys. **129**, 204306 (2008).
[25] A. J. Yencha, M. C. A. Lopes, and G. C. King, Chem. Phys. **279**, 55 (2002).
[26] R. A. Mackie, L. G. Shpinkova, D. M. P. Holland, and D. A. Shaw, Chem. Phys. **288**, 211 (2003).
[27] A. Weaver, D. W. Arnold, S. E. Bradforth, and D. M. Neumark, J. Chem. Phys. **94**, 1740 (1991).
[28] D. B. Atkinson, K. K. Irikura, and J. W. Hudgens, J. Phys. Chem. A **101**, 2045 (1997).
[29] R. L. Hudson and F. Williams, J. Chem. Phys. **75**, 3381 (1976).
[30] G. L. Gutsev, P. Jena, and R. J. Bartlett, Chem. Phys. Lett. **292**, 289 (1998).
[31] D. J. Grant, D. A. Dixon, D. Camaioni, R. G. Potter, and K. O. Christe, Inorg. Chem. **48**, 8811 (2009).
[32] N. N. Greenwood, J. Chem. Soc., 3811 (1959).
[33] S. Riedel, T. Köchner, X. Wang, and L. Andrews, Inorg. Chem. **49**, 7156 (2010).

Table E-1. Behavior of photosensitive product absorptions[a] of a Ne:BF_3:H_2O = 400:1:x sample codeposited at 4.3 K with a beam of discharged neon atoms on subsequent filtered tungsten-lamp (780-520 nm) or mercury-arc (420-280 nm, unfiltered) irradiation.

cm^{-1}	Assign.	Cutoff Wavelength (nm)							
		>780	>695	>630	>520	>420	>345	>280	Unfil.
447.5	$^{11}BF_2OH$								
449.1	$^{10}BF_2OH$								
451.1									–
496.7	$F^{11}BO$	+	+	+	+	++	+	+	+
509.6	$^{11}BF_3^+$	–	–	–	–	–	– –	0	
520.8	BF_2OH								
523.8	$^{11}BF_2$							–	–
525.8									–
529.4	$^{10}BF_2$							–	–
545.9						+	+	+	+
551.0						+	+	+	+
556.8						+	+	+	+
594.4	BF_3^-	–	0						
595.2	BF_3^-	–	0						
618.4						+	+	+	– –
624.2						+	+	+	– –
680.9	$^{11}BF_2OH$								
708.0	$^{10}BF_2OH$								
823.3		+		+		+		+	0
830.4		+		+		+		+	0
847.2	$^{11}BF_2^-$	–	– –	0					

cm^{-1}	Assign.	Cutoff Wavelength (nm)							
		>780	>695	>630	>520	>420	>345	>280	Unfil.
855.7	$^{11}BF_2^-$	– –	– –	0					
871.7	$^{10}BF_2^-$	–	0						
879.3	BF_2OH								
880.7	$^{10}BF_2^-$	– –	0						
959.2	BF_2OH							+	+
1001.8	$^{11}BF_3^-$	– –	– –	0					
1002.2	$^{11}BF_3^-$	– –	– –	0					
1004.7	$^{11}BF_3^-$	–	– –	0					
1021.7	$^{11}BF_3^-$	–	– –	0					
1026.4	$^{11}BF_3^-$	–	– –	0					
1039.0	BF_2OH							+	+
1056.2	$^{10}BF_3^-$	– –	0						
1059.1	$^{10}BF_3^-$	–							0
1061.4	$^{10}BF_3^-$	–	– –	0					
1064.4	BF_4^- ?	+	+	+	+	+	+	++	++
1151.5	$^{11}BF_2$							–	–
1181.6	$^{10}BF_2$							–	–
1400.5	$^{11}BF_2OH$							+	+
1414.9	$^{11}BF_2OH$							+	+
1420.9						0			
1456.9	$^{10}BF_2OH$						+	+	+
1464.2	$^{11}BF_2OH$								
1515.7	$^{10}BF_2OH$							+	+
1661.6	$^{11}BF_2OH^+$	–	–			–	–	– –	0
1722.0	$^{10}BF_2OH^+$							–	0

cm^{-1}	Assign.	Cutoff Wavelength (nm)							
		>780	>695	>630	>520	>420	>345	>280	Unfil.
1790.8	$^{11}BF_3^+$		–	–	–	–	– –	0	
1856.4	$^{10}BF_3^+$		–	–	–	–	– –	0	
2026.0	$^{11}BF_2^+$	+		+	+	+	+	–	– –
2077.3	$F^{11}BO$	+	+	+	+	++	+	+	+
2101.4	$^{10}BF_2^+$	+			+	+	+	–	– –
2150.4	$F^{10}BO$	+	+	+	+	++	+	+	+
2534.0	$^{11}BF_2$							–	–
2612.3	$^{10}BF_2$							–	–
3240.1 3247.2	BF_2OH^+						–	–	0
3712.4	BF_2OH							+	+

[a] Based on previous investigations, the standard uncertainty (type B) in the neon-matrix measurements is 0.1 cm^{-1} (1σ). +,– indicate whether the absorption increases or decreases in intensity on irradiation through the filter with the given cutoff wavelength. A blank indicates that no change occurred, and 0 that the peak is destroyed at that cutoff wavelength. ++ or – – indicates that with the given filter the increase or decrease in the intensity of the peak is exceptionally large.

Table E-2. Behavior on subsequent filtered mercury-arc irradiation of photosensitive product absorptions[a] of Ne:BF_3:H_2O = 400:1:x samples prepared using isotopically enriched H_2O and codeposited at 4.3 K with a beam of discharged neon atoms.

cm^{-1}			Cutoff Wavelength (nm) in $D_2{}^{18}O$ Study			Assignment
H_2O	D_2O	$D_2{}^{18}O$	>345	>280	Unfil.	
		440.2				$^{11}BF_2{}^{18}OH$
		441.9				$^{10}BF_2{}^{18}OH$
447.5	447.5	447.5				$^{11}BF_2{}^{16}OH$
449.1		449.1				$^{10}BF_2{}^{16}OH$
451.1						
		474.1				$^{11}BF_2{}^{18}OD$
		475.7				$^{11}BF_2{}^{18}OD$
	480.0	479.9				$^{11}BF_2{}^{16}OD$
	481.7	481.6				$^{11}BF_2{}^{16}OD$
		493.7	+	+	+	$F^{11}B^{18}O$
496.7	496.7	497.1	+	+	+	$F^{11}B^{16}O$
509.6	509.7	509.5	0			$^{11}BF_3{}^+$
		519.0	+			$^{11}BF_2{}^{18}OH$
520.8	520.8	520.8	+			$^{11}BF_2{}^{16}OH$
523.8	523.8	523.8	–	–	–	$^{11}BF_2$
525.8						
529.4	529.4	529.4	–	–	–	$^{10}BF_2$
545.9	546.0	545.6	+	+	+	
551.0	550.9	550.9	+	+	+	
556.8	557.2	556.4	+	+	+	

cm^{-1}			Cutoff Wavelength (nm) in $D_2{}^{18}O$ Study			Assignment
H_2O	D_2O	$D_2{}^{18}O$	>345	>280	Unfil.	
594.4[b]	594.4	594.4	0			BF_3^-
595.2[b]	595.2	595.2	0			BF_3^-
618.4		618.7vw			0	
624.2						
	677.9	678.0				$^{11}BF_2{}^{18}OD$
	680.4	680.8				$^{11}BF_2{}^{16}OD$
680.9						$^{11}BF_2OH$
	705.2	705.2				$^{10}BF_2{}^{18}OD$
		705.6				$^{10}BF_2{}^{18}OH$
	707.6	707.6				$^{10}BF_2{}^{16}OD$
708.0	708.0	708.0				$^{10}BF_2{}^{16}OH$
	743.4	743.4	+	+	+	$BF_2{}^{18}OD$
	751.2	751.2	+	+	+	$BF_2{}^{16}OD$
	756.5		0			
	757.0		0			
	770.3		0			
	771.4		0			
	781.7	781.7	+	+	+	$BF_2{}^{18}OD$
	787.6	787.7	+	+	+	$BF_2{}^{16}OD$
823.3	823.3	823.3	+	+	0	
830.4	830.5				0	
	843.3	843.3	0			
847.2[b]	847.3[b]	847.3	0			$^{11}BF_2^-$
855.7[b]	855.6[b]	855.6	0			$^{11}BF_2^-$

cm^{-1}			Cutoff Wavelength (nm) in $D_2{}^{18}O$ Study			Assignment
H_2O	D_2O	$D_2{}^{18}O$	>345	>280	Unfil.	
		863.0				$^{11}BF_2{}^{18}OD$
		864.8				$^{11}BF_2{}^{18}OH$
871.7[b]	871.6[b]	871.5[b]	0			$^{10}BF_2^-$
879.3	879.3	879.2				$BF_2{}^{16}OH$, $BF_2{}^{16}OD$
880.7[b]	880.7[b]	880.5[b]	0			$^{10}BF_2^-$
	884.0	884.0				
	951.7	951.7	+		+	$^{11}BF_2{}^{18}OH$
959.2	959.2	959.2	+		+	$^{11}BF_2{}^{16}OH$
1001.8[b]	1001.9[b]	1001.8[b]	0			$^{11}BF_3^-$
1002.2[b]	1002.3[b]	1002.2[b]	0			$^{11}BF_3^-$
1004.7[b]	1004.7[b]	1004.7[b]	0			$^{11}BF_3^-$
	1010.4		+	+	+	
	1018.7		+	+	+	
1021.7[b]	1021.7[b]	1021.7[b]	0			$^{11}BF_3^-$
1026.4[b]	1026.3[b]	1026.3[b]	0			$^{11}BF_3^-$
		1027.6	+		+	
		1035.2	+		+	$^{11}BF_2{}^{18}OH$
1039.0	1039.0	1039.1	+		+	$^{11}BF_2{}^{16}OH$
1056.2[b]	1056.0[b]	1056.1[b]	0			$^{10}BF_3^-$
1059.1		1058.8			0	
1061.4[b]	1061.4[b]	1061.4[b]	0			$^{10}BF_3^-$
1064.4		1064.5vw			+	BF_4^- ?
1151.5	1151.4	1151.5		–	–	$^{11}BF_2$
1181.6	1181.6	1181.6		–	–	$^{10}BF_2$

cm^{-1}			Cutoff Wavelength (nm) in $D_2{}^{18}O$ Study			Assignment
H_2O	D_2O	$D_2{}^{18}O$	>345	>280	Unfil.	
		1389.2	+		+	$^{11}BF_2{}^{18}OH$
		1394.0	+		+	$^{11}BF_2{}^{18}OH$
		1396.6	+		+	$^{11}BF_2{}^{18}OD$
1400.5	1400.5	1400.5	+		+	$^{11}BF_2{}^{16}OH$
	1400.9	1400.8	+		+	$^{11}BF_2{}^{16}OH$
	1405.9	1405.9	+		+	$^{11}BF_2{}^{16}OD$
1414.9	1414.9	1414.9	+		+	$^{11}BF_2{}^{16}OH$
	1442.3				-	
		1451.4				$^{10}BF_2{}^{18}OD$
	1453.6	1453.6sh				$^{10}BF_2{}^{16}OD$
1456.9	1456.6	1456.9	+		+	$^{10}BF_2{}^{16}OH$, $^{10}BF_2{}^{16}OD$
1464.2	1464.2	1464.2	+		+	$^{11}BF_2OH$
	1505.4					$^{10}BF_2{}^{16}OD$
		1506.5	+		+	$^{10}BF_2{}^{18}OH$
1515.7	1515.7	1515.7	+		+	$^{10}BF_2{}^{16}OH$
1661.6	1662.3	1662.1	-	-	0	$^{11}BF_2OH^+$, $^{11}BF_2OD^+$
1722.0	1721.0	1721.3	-	-	0	$^{10}BF_2OH^+$, $^{10}BF_2OD^+$
1790.8	1790.9	1790.7	-	0		$^{11}BF_3{}^+$
1856.4	1855.3vw	1855.8vw	0			$^{10}BF_3{}^+$
2026.0	2026.0	2026.0	+	+	-	$^{11}BF_2{}^+$
	2050.6	2050.6	+	+	+	$F^{11}B^{18}O$
2077.3	2077.3	2077.3	+	+	+	$F^{11}B^{16}O$
2101.4	2101.3	2101.4	+	+	-	$^{10}BF_2{}^+$
	2123.1	2123.1	+	+	+	$F^{10}B^{18}O$

cm^{-1}			Cutoff Wavelength (nm) in $D_2{}^{18}O$ Study			Assignment
H_2O	D_2O	$D_2{}^{18}O$	>345	>280	Unfil.	
2150.4	2150.4	2150.4	+	+	+	$F^{10}B^{16}O$
	2395.7	2395.9vw	–	–	0	$BF_2{}^{16}OD^+$
	2401.3	2401.3vw	–	–	0	$BF_2{}^{16}OD^+$
2534.0	2534.0	2534.0	+	–	–	$^{11}BF_2$
2612.3	2612.2	2612.2	+	–	–	$^{10}BF_2$
	2720.3	2720.2	+		+	$BF_2{}^{18}OD$
	2737.1	2737.1	+		+	$BF_2{}^{16}OD$
		3229.1	–	–	0	$BF_2{}^{18}OH^+$
		3236.8	–	–	0	$BF_2{}^{18}OH^+$
3240.1	3239.6	3239.7	–	–	0	$BF_2{}^{16}OH^+$
3247.2	3246.8vw	3246.3vw	–	–	0	$BF_2{}^{16}OH^+$
	3700.9	3700.8	+		+	$BF_2{}^{18}OH$
3712.4	3712.4	3712.4	+		+	$BF_2{}^{16}OH$

[a] Based on previous investigations, the standard uncertainty (type B) in the neon-matrix measurements is 0.1 cm^{-1} (1σ). +,– indicate whether the absorption increases or decreases in intensity on irradiation through the filter with the given cutoff wavelength. A blank indicates that no change occurred, and 0 that the peak is destroyed at that cutoff wavelength.

[b] Destroyed by radiation of wavelength > 420 nm.